IEEE Access
Multidisciplinary ⋮ Rapid Review ⋮ Open Access Journal

Received 19 February 2026, accepted 29 March 2026, date of publication 1 April 2026, date of current version 6 April 2026.

Digital Object Identifier 10.1109/ACCESS.2026.3679688

RESEARCH ARTICLE

Two-Level Beam Selection Algorithm for mmWave Wireless Power Transfer Systems: Training Overhead Reduction and Performance Analysis

SEUNGSU CHUNG[1], JAEYEON HA[1], JAEHYUN PARK[1], (Member, IEEE), JAE CHEOL PARK[2], AND JUNGICK MOON[2], (Member, IEEE)

[1]Department of Electronic Engineering, Pukyong National University, Busan 48513, South Korea
[2]Electronics and Telecommunications Research Institute (ETRI), Daejeon 34129, South Korea

Corresponding author: Jaehyun Park (jaehyun@pknu.ac.kr)

This work was supported by the Institute of Information and Communications Technology Planning and Evaluation (IITP) Grant funded by Korean Government through MSIT (Development of Multi-Meter Level Radio Beam Wireless Charging Technology Based on Millimeter Waves) under Grant RS-2024-00398981.

ABSTRACT Millimeter-wave (mmWave) wireless power transfer (WPT) systems require efficient beam selection algorithms to maximize energy harvesting at wireless charging devices (WCDs). The conventional exhaustive codebook search method, while optimal, requires significant training overhead that reduces the time available for actual power transfer. This paper proposes a novel two-level beam selection algorithm that significantly reduces the training time slots while maintaining near-optimal energy harvesting performance. The proposed algorithm employs a hierarchical approach: first, it uses sum beams to identify the angle group containing the optimal beam direction, and then applies difference beams with decision statistics based on the difference-to-sum ratio (DSR) to determine the final beam selection within the identified group. We provide a comprehensive analytical framework using detection theory to characterize the beam selection error probability. Furthermore, we develop an optimal resource allocation framework that determines the optimal number of beams to maximize harvested energy by exploiting the concavity property of the harvested energy function. A bisection-based optimization algorithm is proposed to efficiently find the optimal solution. Simulation results demonstrate that the proposed algorithm achieves higher harvested energy compared to the exhaustive codebook search method by reducing training overhead.

INDEX TERMS Wireless power transfer, millimeter-wave communications, beam selection, monopulse radar, energy harvesting.

I. INTRODUCTION

The rapid proliferation of Internet of Things (IoT) devices and wireless sensor networks has created an unprecedented demand for sustainable and efficient power solutions. Wireless power transfer (WPT) technology has emerged as a promising solution to address the energy constraints of battery-powered devices, particularly in scenarios where battery replacement is impractical or impossible. Among various WPT technologies, radio frequency (RF) energy harvesting has gained significant attention due to its flexibility and ability to provide power over extended distances [1], [2] and references therein.

Millimeter-wave (mmWave) frequencies offer unique advantages for WPT systems, including abundant spectrum availability, high power density, and excellent directivity through beamforming techniques [3], [4], [5]. However, the high path loss and sensitivity to blockage inherent in mmWave propagation necessitate precise beam alignment between the wireless charging station (WCS) and

The associate editor coordinating the review of this manuscript and approving it for publication was Ahmed Almradi.

wireless charging devices (WCDs) to achieve efficient power transfer.

The conventional approach to optimal beam selection in mmWave WPT systems relies on exhaustive codebook search algorithms, which systematically evaluate all possible beam directions to identify the one that maximizes the received signal strength at the WCD [6], [7], [8]. While this method guarantees optimal performance, it comes with a significant drawback: the extensive training overhead required to test all beam candidates reduces the time available for actual power transfer, thereby limiting the overall energy harvesting efficiency.

Recent research has explored various approaches to design beamforming weight and reduce beam training overhead in mmWave communication systems. Hierarchical beam codebook design and search algorithms [8], [9], compressed sensing-based methods [10], and machine learning approaches [11] have been proposed to accelerate the mmWave beamforming process. Especially, data-driven approaches leveraging Deep Learning (DL) have been actively explored to accelerate beam alignment [12], [13], [14]. For instance, in [12], the optimal beam selection framework employing Deep Neural Networks (DNN) is proposed for 6G environment and in [13], out-of-band information, such as LiDAR and position data, is utilized with Convolutional Neural Networks (CNNs) to aid beam selection. While these learning-based methods demonstrate promising performance, they generally necessitate extensive offline datasets for training and considerable computational resources for inference, which may not be feasible for resource-constrained WPT receivers. Therefore, in this paper, we focus on a signal processing-based approach that achieves rapid beam alignment without the burden of pre-training data or high computational complexity.

Furthermore, most of existing fast beam alignment solutions [9], [10], [15] are designed for communication systems where the primary objective is to maximize data throughput. In such systems, high computational complexity or multi-stage training overhead is often tolerated to achieve precise alignment. In contrast, for WPT systems—particularly those powering simple IoT devices—the energy constraints are severe, and the receiver architecture must remain simple. Consequently, applying communication-centric beam selection methods directly to WPT can be suboptimal because the training overhead consumes valuable time that could otherwise be used for energy harvesting. Therefore, there is a critical need for a WPT-specific beam selection strategy that minimizes training overhead and computational complexity to maximize the end-to-end harvested energy, even at the cost of slight beam misalignment.

In this paper, we propose a novel two-level beam selection algorithm specifically designed for mmWave WPT systems. Our approach draws inspiration from monopulse radar techniques, which have been extensively used in target tracking and direction-finding applications [16], [17], [18], [19], [20]. The key insight is that by using sum and difference beam patterns, we can efficiently narrow down the search space and identify the optimal beam direction with significantly fewer training time slots. The main contributions of this paper are as follows:

- We propose a two-level hierarchical beam selection algorithm that reduces the training overhead from N_b time slots (required by exhaustive codebook search) to approximately $\lceil N_b/L \rceil + 1$ time slots while maintaining near-optimal energy harvesting performance. Here, L is the number of beam weights in one group.
- We develop a comprehensive analytical framework based on detection theory and order statistics to characterize the beam selection error probability in the presence of additive white Gaussian noise (AWGN). Our analysis properly addresses the multi-hypothesis testing nature of the problem, avoiding the common error of simply summing pairwise confusion probabilities.
- We demonstrate through extensive simulations that the proposed algorithm achieves higher overall harvested energy compared to the exhaustive codebook search method, despite potential beam selection errors, due to the significant reduction in training overhead.
- From the analytic results, the performance trade-offs is discussed, enabling the optimization of the proposed algorithm for specific deployment scenarios. Accordingly, we propose an optimal resource allocation framework that determines the optimal number of beams N_b^* to maximize harvested energy. We prove the concavity of the harvested energy function and develop a bisection-based optimization algorithm to efficiently find the optimal solution.

The remainder of this paper is organized as follows. Section II presents the system model and problem formulation. Section III describes the proposed two-level beam selection algorithm in detail. Section IV provides the theoretical analysis of beam selection error probability using detection theory. Section V presents the optimal resource allocation framework for maximizing harvested energy. Section VI presents simulation results and performance comparisons. Finally, Section VII concludes the paper.

II. SYSTEM MODEL AND PROBLEM FORMULATION

A. SYSTEM ARCHITECTURE

As illustrated in Fig. 1, we consider a mmWave WPT system consisting of a WCS equipped with a uniform linear antenna array (ULA) of M antenna elements and a WCD with a single antenna element. The WCS is responsible for transmitting RF energy signals to the WCD, which harvests electrical energy from the received RF signals to power IoT sensors or other low-power devices.

The WCS employs digital beamforming with a predefined codebook of beamforming vectors. This approach is practical for WPT applications as it allows for efficient hardware implementation while providing sufficient beamforming gain for energy transfer. The predefined beam set is denoted as

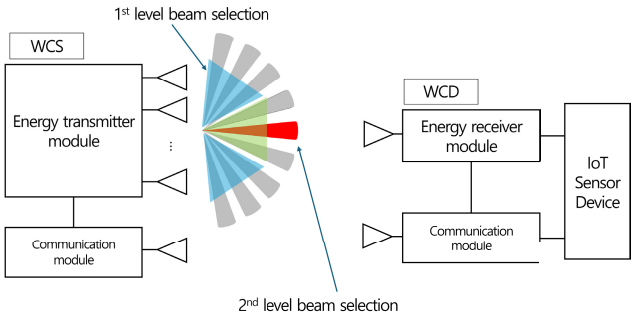

FIGURE 1. The mmWave WPT system with two-level beam selection algorithm.

$\mathcal{W} = \{w_1, w_2, \ldots, w_{N_b}\}$, where N_b is the total number of beamforming vectors in the codebook.

B. CHANNEL MODEL

Due to the directional nature of mmWave propagation and the high path loss, we consider a line-of-sight (LoS) dominant channel model. The channel vector from the WCS to the WCD is given by:

$$h = \sqrt{\rho_p}\, a(\theta_D), \tag{1}$$

where ρ_p represents the large-scale path loss, $\theta_D \in [-\pi/2, \pi/2]$ is the angle-of-departure (AoD) from the WCS to the WCD, and $a(\theta_D)$ is the array response vector defined as:

$$a(\theta_D) = \frac{1}{\sqrt{M}}[1, e^{j2\pi \frac{d}{\lambda} \sin\theta_D}, \ldots, e^{j2\pi \frac{d}{\lambda}(M-1)\sin\theta_D}]^T, \tag{2}$$

where d is the antenna spacing (typically $d = \lambda/2$), and λ is the wavelength.

C. BEAMFORMING CODEBOOK DESIGN

The beamforming vectors in the codebook are designed to provide uniform coverage over the angular range $[-\Theta_M, \Theta_M]$, where Θ_M determines the angle coverage of WCS. Each beamforming vector is given by:

$$w_i = a(\theta_i), \tag{3}$$

where θ_i is selected from the predefined angle set:

$$\Theta = \left\{ \theta_i \middle| \theta_i = -\Theta_M + \Delta_\theta (i-1), i = 1, \ldots, N_b \right\}, \tag{4}$$

with $\Delta_\theta = \frac{2\Theta_M}{N_b - 1}$ being the angular spacing between adjacent beams.

D. SIGNAL MODEL

The received signal at the WCD when the WCS transmits using beamforming vector w_i is:

$$y_i = \sqrt{P_t} h^H w_i s + n_i, \tag{5}$$

where P_t is the transmit power, s is the transmitted signal with $\mathbb{E}[|s|^2] = 1$, and n_i is the AWGN with zero mean and variance σ_n^2. Substituting the channel model, the received signal becomes:

$$y_i = \sqrt{P_t \rho_p}\, a^H(\theta_D) w_i s + n_i. \tag{6}$$

The beamforming gain achieved by the ith beamforming vector is:

$$G_i = |a^H(\theta_D) w_i|^2 = \left| \frac{\sin\left(\frac{M\pi}{2}(\sin\theta_D - \sin\theta_i)\right)}{\sin\left(\frac{\pi}{2}(\sin\theta_D - \sin\theta_i)\right)} \right|^2. \tag{7}$$

E. ENERGY HARVESTING MODEL

We consider a frame-based transmission structure where each frame consists of K time slots, each with duration T_s seconds. Out of these K time slots, K_p slots are allocated for beam training, and the remaining $K - K_p$ slots are used for energy transfer using the selected beamforming vector.

Throughout the paper, the practical nonlinear EH model in [21] and [22] is considered. Assuming that the additive thermal noise at the receiver is negligible compared to the beamforming signal, the total harvested energy in one frame is:

$$E_i = (K - K_p) T_s \left(\frac{\Psi - M_{\text{EH}}\, \Omega}{1 - \Omega} \right) \tag{8}$$

where

$$\Omega = \frac{1}{1 + \exp(ab)}, \qquad \Psi = \frac{M_{\text{EH}}}{1 + \exp[-a(P_{in} - b)]}. \tag{9}$$

Here, Ψ represents a logistic-type nonlinear RF-to-DC conversion function with respect to the received power P_{in}, which is given by

$$P_{\text{in}} = P_t\, \rho_p\, G_i \tag{10}$$

where G_i is the beamforming gain when the i-th beam is selected.

Additionally, M_{EH} is the maximum power harvested by the energy harvesting (EH) receiver when the module is saturated. The parameters a and b are related to the detailed EH circuit specifications.

F. PROBLEM FORMULATION

The objective is to maximize the harvested energy by selecting the optimal beamforming vector while minimizing the training overhead. The conventional exhaustive codebook search approach solves:

$$i^* = \arg \max_{i \in \{1,2,\ldots,N_b\}} |y_i|^2, \tag{11}$$

which requires $K_p = N_b$ training time slots.

Our goal is to develop an algorithm that can identify the near-optimal beam with $K_p \ll N_b$ training time slots, thereby maximizing the overall harvested energy:

$$\max_i \; E_i = (K - K_p) T_s \left(\frac{\Psi - M_{\text{EH}}\, \Omega}{1 - \Omega} \right). \tag{12}$$

From (9) and (10), it is evident that maximizing the beamforming gain G_i is essential for maximizing the harvested energy.

III. PROPOSED TWO-LEVEL BEAM SELECTION ALGORITHM

This section presents the proposed two-level beam selection algorithm, which significantly reduces the training overhead while maintaining near-optimal performance. The algorithm is inspired by monopulse radar techniques and consists of two hierarchical stages: coarse group identification using sum beams, followed by fine beam selection using difference beams.

A. ALGORITHM OVERVIEW

The key insight behind our approach is to partition the angular space into overlapping groups and use specially designed beam patterns to efficiently identify the optimal beam. Instead of testing all N_b individual beams, we first identify which group contains the optimal beam direction, then determine the specific beam within that group.

The algorithm operates in two stages:

- **Level 1 (Angular Group Identification):** Use sum beams to identify the angular group containing the optimal beam direction.
- **Level 2 (Fine Beam Selection):** Use difference beams and decision statistics to select the optimal beam within the identified group.

B. LEVEL 1: ANGULAR GROUP IDENTIFICATION

1) GROUP FORMATION

We partition the predefined angle set Θ into N_g groups of adjacent angles. For simplicity, we assume each group contains L adjacent angles (except possibly the boundary groups). The groups are defined as:

$$\Theta_g = \{\theta_{(g-1)L+1}, \theta_{(g-1)L+2}, \ldots, \theta_{\min(gL,N_b)}\}, \tag{13}$$

where $g = 1, 2, \ldots, N_g$ and $N_g = \lceil N_b/L \rceil$.

2) SUM BEAM DESIGN

For each group Θ_g, we define a sum beam that provides broad coverage over the angular range of the group, which is used for the group identification. The sum beam for group g is designed as:

$$w_{\Sigma,g} = \frac{1}{\sqrt{|\Theta_g|}} \sum_{\theta_i \in \Theta_g} a(\theta_i), \tag{14}$$

where $|\Theta_g|$ is the cardinality of group Θ_g.

This design ensures that the sum beam has significant gain over the entire angular range of the group while suppressing interference from other directions. Furthermore, because it does not require any modification of predefined selection beam weights, the proposed algorithm can be applied to conventional selection beamforming RF modules.

3) GROUP SELECTION

During the first level of training, the WCS sequentially transmits using sum beams $w_{\Sigma,g}$ for $g = 1, 2, \ldots, N_g$.

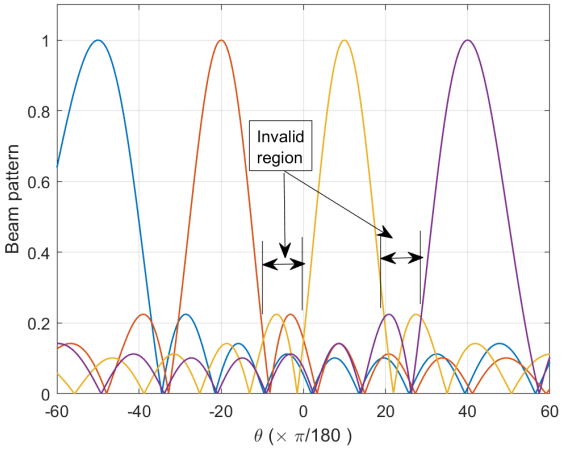

(a)

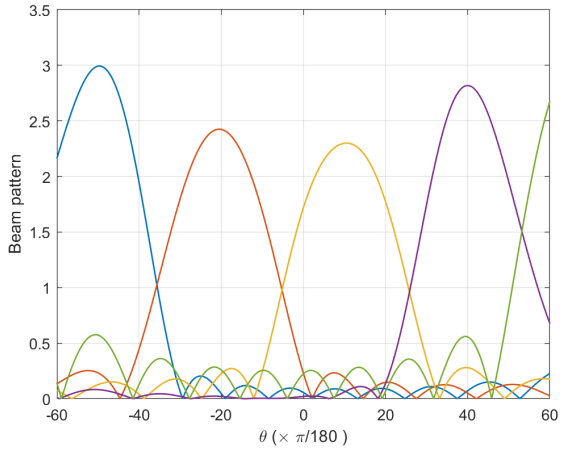

(b)

FIGURE 2. Beam pattern of (a) w_i with $\theta_i = \{-50, -20, 10, 40\} \times \frac{\pi}{180}$ and (b) $w_{\Sigma,g}$ with $g = \{2, 3, 4, 5\}$.

The WCD measures the received signal strength for each sum beam:

$$y_{\Sigma,g} = \sqrt{P_t \rho_p} a^H(\theta_D) w_{\Sigma,g} s + n_g. \tag{15}$$

The optimal group is selected as:

$$g^* = \arg \max_{g \in \{1,2,\ldots,N_g\}} |y_{\Sigma,g}|^2. \tag{16}$$

The group identification stage requires $N_g = \lceil N_b/L \rceil$ training time slots.

Fig. 2 (a) illustrates the beam patterns of individual beams, while Fig. 2 (b) shows the sum beam patterns for different groups, when $\Theta_M = \frac{\pi}{2}$, $\Delta_\theta = \frac{\pi}{18}$ and the predefined angle set is given as $\Theta = \left\{\frac{\pi}{180}(-90 : 10 : 90)\right\}$. If we group three adjacent angles, we can have seven angle groups as follows:

$$\begin{aligned}\Theta &= \{\Theta_1, \Theta_2, \ldots, \Theta_7\} \\ &= \frac{\pi}{180}\{(-90, -80, -70), (-60, -50, -40), (-30, \\ &\quad -20, -10), (0, 10, 20), (30, 40, 50), (60, 70, 80), (90)\}.\end{aligned} \tag{17}$$

We note that if the beamforming weight with a center angle in each group is utilized to determine the group selection, shown in Fig. 2 (a), the group index is incorrectly determined due to the side-lobe leakage, referred to as "invalid region." For example, for $\Theta_4 \in (0, 10, 20)$, $|a^H(\theta_D)w_{11}|^2 < |a^H(\theta_D)w_8|^2$ for $\theta_D \in \left[-\frac{5\pi}{180}, 0\right]$, where $w_8 = a\left(-\frac{20\pi}{180}\right)$ and $w_{11} = a\left(\frac{10\pi}{180}\right)$. In Fig. 2 (b), the beam patterns of $\bar{w}_{\Sigma,g}$ with $g = \{2, 3, 4, 5\}$ are illustrated. It can be found that there is no invalid region.

Remark 1: The group size L is a design parameter that determines the trade-off between training overhead and beam selection reliability. A larger L reduces the Level 1 overhead by decreasing the number of groups N_g. However, it also widens the sum beam, leading to a reduction in beamforming gain (spreading loss) and potentially decreasing the group detection probability at low SNRs. Conversely, a smaller L yields higher gain and precision but results in higher overhead. In this paper, we adopt $L = 3$ as a representative value that achieves a substantial reduction in overhead while maintaining robust beam selection performance. However, the proposed algorithm is generic and can be extended to any integer L depending on the specific system requirements and SNR conditions.

C. LEVEL 2: FINE BEAM SELECTION USING DIFFERENCE BEAMS

Once the optimal group g^* is identified, we need to determine which specific beam within Θ_{g^*} provides the best performance. This is achieved using difference beams and decision statistics based on the difference-to-sum ratio (DSR).

1) DIFFERENCE BEAM DESIGN

The difference beam for group g^* is designed to provide directional information within the group. Inspired by monopulse radar, the difference beam is constructed as:

$$w_{\Delta,g^*} = \frac{1}{2}\left(a(\theta_{(g^*-1)L+1}) - a(\theta_{\min(g^*L,Nb)})\right). \tag{18}$$

The difference beam has a null at the center of the angular group and exhibits opposite polarities on either side of the null. This property enables fine discrimination between different angular positions within the group.

2) DSR COMPUTATION

The WCS transmits using the difference beam $w_{\Delta,\hat{g}}$, and the WCD receives:

$$y_{\Delta,\hat{g}} = \sqrt{P_t \rho_p} a^H(\theta_D) w_{\Delta,\hat{g}} s + n_\Delta. \tag{19}$$

The DSR is then computed as:

$$\text{DSR} = \frac{y_{\Delta,\hat{g}}}{y_{\Sigma,\hat{g}}}. \tag{20}$$

The DSR provides information about the relative position of the true AoD within the selected group. Fig. 1 illustrates the DSR values as a function of the true AoD for a specific group. Specifically, the DSR is evaluated for $\theta_D \in \frac{\pi}{180}[-35, -5]$ with $\bar{w}_{\Sigma,3}$ and $\bar{w}_{\Delta,3}$.

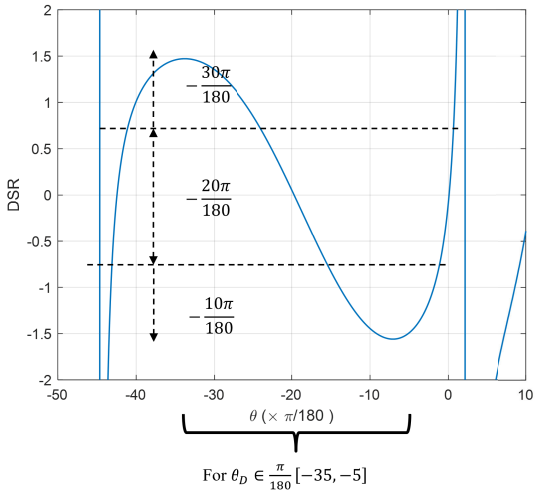

FIGURE 3. DSR values for $\theta_D \in \frac{\pi}{180}[-35, -5]$ with $\bar{w}_{\Sigma,3}$ and $\bar{w}_{\Delta,3}$.

3) DECISION RULES

Based on the DSR value, the WCD makes a decision about which beam to select from group Θ_{g^*}. For a group with three beams $\{w_{3(g^*-1)+1}, w_{3(g^*-1)+2}, w_{3g^*}\}$, the decision rules are:

$$i^* = \begin{cases} \text{index of } w_{3(g^*-1)+1} & \text{if DSR} \le -\tau, \\ \text{index of } w_{3(g^*-1)+2} & \text{if } -\tau < \text{DSR} < \tau, \\ \text{index of } w_{3g^*} & \text{if DSR} \ge \tau, \end{cases} \tag{21}$$

where τ is a decision threshold magnitude that can be optimized based on the system parameters such as sum and difference beam patterns. Note that τ corresponds to the symmetric decision boundary derived from the detection theory analysis in Section IV-A.

D. ALGORITHM SUMMARY

Algorithm 1 summarizes the complete two-level beam selection procedure. The total training overhead is given as

$$K_p = N_g + 1 = \lceil N_b/3 \rceil + 1, \tag{22}$$

which is significantly less than the N_b time slots required by exhaustive codebook search.

Remark 2: While this paper focuses on a quasi-static channel model, the proposed two-level algorithm can be extended to support mobile WCDs. For a moving WCD, the validity of the selected beam is maintained if the angular change $\Delta\theta$ within a frame duration remains within the beamwidth. For low-mobility scenarios, the algorithm can operate in a "Tracking Mode". Specifically, assuming the optimal group index g^* changes slowly, the WCS can skip the Level 1 (group identification) stage and only perform Level 2 (fine selection) using the previous group index. This allows for continuous beam tracking with minimal overhead.

Algorithm 1 Two-Level Beam Selection Algorithm

Input: Predefined beam set $\{w_1, \ldots, w_{N_b}\}$, number of groups N_g
Level 1: Group Identification
for $g = 1$ to N_g **do**
    WCS transmits using sum beam $w_{\Sigma,g}$
    WCD measures $|y_{\Sigma,g}|^2$
end for
Select optimal group: $g^* = \arg\max_g |y_{\Sigma,g}|^2$
Level 2: Fine Selection
WCS transmits using difference beam w_{Δ,g^*}
WCD measures y_{Δ,g^*}
Compute DSR: DSR $= y_{\Delta,g^*}/y_{\Sigma,g^*}$
Apply decision rules to select i^*
Output: Selected beam index i^*

It can be extended to a multi-frame structure. For high-mobility scenarios, the DSR metric can be fed into sequential estimation frameworks, such as Kalman filters, to predict the WCD's trajectory and angular velocity. That is, the proposed scheme can be flexibly integrated into multi-frame protocols depending on the mobility conditions. A detailed performance analysis of these tracking extensions is beyond the scope of this paper and remains a topic for future work.

IV. PERFORMANCE ANALYSIS ON TWO-LEVEL BEAM SELECTION ALGORITHM

A. ANALYSIS ON BEAM SELECTION ERROR PROBABILITY

This section provides a comprehensive analytical framework for characterizing the beam selection error probability of the proposed two-level algorithm. We employ detection theory principles to model the decision-making process and derive closed-form expressions for the error probabilities in both levels of the algorithm.

1) LEVEL 1 ANALYSIS: GROUP SELECTION ERROR PROBABILITY

The group selection process in Level 1 can be formulated as a multiple hypothesis testing problem. Let H_g denote the hypothesis that the true AoD θ_D belongs to group Θ_g. The received signal for each sum beam transmission is given as

$$y_{\Sigma,g} = \begin{cases} \sqrt{P_t \rho_p} a^H(\theta_D) w_{\Sigma,g} s + n_g & \text{under } H_g, \\ \sqrt{P_t \rho_p} a^H(\theta_D) w_{\Sigma,j} s + n_j & \text{under } H_j, j \neq g. \end{cases} \tag{23}$$

For the true group (hypothesis H_g), the signal-to-noise ratio (SNR) is then given as

$$\text{SNR}_g = \frac{P_t \rho_p |a^H(\theta_D) w_{\Sigma,g}|^2}{\sigma_n^2}. \tag{24}$$

For interfering groups (hypothesis $H_j, j \neq g$), the SNR is given as

$$\text{SNR}_j = \frac{P_t \rho_p |a^H(\theta_D) w_{\Sigma,j}|^2}{\sigma_n^2}. \tag{25}$$

The probability of incorrectly selecting group j instead of the true group g is given as

$$P_{g \to j} = \Pr(|y_{\Sigma,j}|^2 > |y_{\Sigma,g}|^2 | H_g). \tag{26}$$

The following lemma provides a closed-form approximation for this probability under high SNR conditions.

Lemma 1: Under the assumption of Gaussian noise and high SNR conditions, the pairwise confusion probability between groups g and j can be approximated as:

$$\begin{aligned} P_{g \to j} &= Q\left(\frac{\text{SNR}_g - \text{SNR}_j}{\sqrt{2(1 + \text{SNR}_g + \text{SNR}_j)}} \right) \\ &\approx Q\left(\frac{\text{SNR}_g - \text{SNR}_j}{\sqrt{2(\text{SNR}_g + \text{SNR}_j)}} \right). \end{aligned} \tag{27}$$

The detailed proof of Lemma 1 is provided in Appendix. Note that this represents the conditional probability of selecting group j given that the true group is g. From Lemma 1, the group selection error probability can then be derived as

$$\begin{aligned} &P_{e,\text{group}} \\ &= \int_{-\Theta_M}^{\Theta_M} p(\theta_D) \cdot P(\text{error}|\theta_D)\, d\theta_D, \\ &\approx \int_{-\Theta_M}^{\Theta_M} p(\theta_D) \cdot \left(P_{g \to g-1} + P_{g \to g+1} \right) d\theta_D. \\ &\approx \frac{1}{2\Theta_M} \int_{-\Theta_M}^{\Theta_M} Q\left(\frac{\text{SNR}_g - \max\limits_{j \neq g} \text{SNR}_j}{\sqrt{2\left(\text{SNR}_g + \max\limits_{j \neq g} \text{SNR}_j \right)}} \right) d\theta_D. \end{aligned} \tag{28}$$

We note that SNR_g and SNR_j are the effective SNRs for the sum beams of groups g and j, respectively in (24) and (25).

2) LEVEL 2 ANALYSIS: FINE BEAM SELECTION ERROR PROBABILITY

Given that the correct group g^* has been identified, the fine beam selection depends on the DSR value. The DSR can be written as

$$\text{DSR} = \frac{\sqrt{P_t \rho_p} a^H(\theta_D) w_{\Delta,g^*} s + n_\Delta}{\sqrt{P_t \rho_p} a^H(\theta_D) w_{\Sigma,g^*} s + n_\Sigma}. \tag{29}$$

For high SNR conditions (i.e., $|\sqrt{P_t \rho_p} a^H(\theta_D) w_{\Sigma,g^*} s| \gg |n_\Sigma|$), the DSR can be approximated as

$$\text{DSR} \approx \frac{a^H(\theta_D) w_{\Delta,g^*}}{a^H(\theta_D) w_{\Sigma,g^*}} + \frac{n_\Delta}{a^H(\theta_D) w_{\Sigma,g^*} s \sqrt{P_t \rho_p}}. \tag{30}$$

The first term represents the deterministic component, while the second term represents the noise contribution. Therefore, DSR follows a Gaussian distribution as DSR $\sim \mathcal{N}\left(\frac{a^H(\theta_D) w_{\Delta,\hat{g}}}{a^H(\theta_D) w_{\Sigma,g^*}}, \frac{\sigma_n^2}{|a^H(\theta_D) w_{\Sigma,g^*} s \sqrt{P_t \rho_p}|^2} \right)$. Importantly, the mean

and variance of the DSR depend only on the true AoD θ_D. Let us denote:

$$\mu(\theta_D) = \frac{a^H(\theta_D)w_{\Delta,g^*}}{a^H(\theta_D)w_{\Sigma,g^*}} \tag{31}$$

$$\sigma^2(\theta_D) = \frac{\sigma_n^2}{|a^H(\theta_D)w_{\Sigma,g^*}s\sqrt{P_t\rho_p}|^2}. \tag{32}$$

The fine beam selection within group $\Theta_{g^*} = \{\theta_{3(g^*-1)+1}, \theta_{3(g^*-1)+2}, \theta_{3g^*}\}$ can be formulated as a three-hypothesis testing problem:

$$H_1: \quad \theta_D \text{ is closest to } \theta_{3(g^*-1)+1} \tag{33}$$

$$H_2: \quad \theta_D \text{ is closest to } \theta_{3(g^*-1)+2} \tag{34}$$

$$H_3: \quad \theta_D \text{ is closest to } \theta_{3g^*} \tag{35}$$

Considering the maximum-likelihood (ML) approach, we assume that under hypothesis H_i, the true AoD θ_D is most likely to be equal to θ_i. Therefore, the likelihood of observing DSR value d under hypothesis H_i is:

$$L(d|H_i) = \frac{1}{\sqrt{2\pi\sigma^2(\theta_i)}} \exp\left(-\frac{(d-\mu(\theta_i))^2}{2\sigma^2(\theta_i)}\right), \tag{36}$$

where $\mu(\theta_i)$ and $\sigma^2(\theta_i)$ are the mean and variance of the DSR when the true AoD is θ_i. Therefore, the optimal decision thresholds τ_1 and τ_2 (with $\tau_1 > \tau_2$) can be derived using the ML ratio test. The ML decision rule is:

$$i^* = \arg\max_{i\in\{1,2,3\}} L(\text{DSR}|H_i). \tag{37}$$

This is equivalent to the threshold-based decision rule:

$$i^* = \begin{cases} 1 & \text{if DSR} > \tau_1 \\ 2 & \text{if } \tau_2 < \text{DSR} \le \tau_1 \\ 3 & \text{if DSR} \le \tau_2 \end{cases} \tag{38}$$

where the optimal thresholds are determined by the intersections of the likelihood functions:

$$\tau_1 = \frac{\mu(\theta_1)+\mu(\theta_2)}{2}, \tag{39}$$

$$\tau_2 = \frac{\mu(\theta_2)+\mu(\theta_3)}{2}. \tag{40}$$

For the symmetric case where the angular spacing is uniform and the beams are equally spaced, we have $\mu(\theta_2) = 0$ (center beam), $\mu(\theta_1) = -\mu(\theta_3)$, which gives:

$$\tau_1 = \tau, \quad \tau_2 = -\tau, \tag{41}$$

where $\tau = \frac{|\mu(\theta_3)|}{2}$ corresponds to the symmetric boundaries used in Algorithm 1.

The probability of error in fine beam selection, given that the correct group has been identified, depends on the true AoD θ_D within the group. Specifically, for a given true AoD θ_D, the error probability is:

$$P_{e,\text{fine}}(\theta_D) = 1 - P(\text{correct selection}|\theta_D), \tag{42}$$

where the correct selection probability depends on which beam is actually optimal for the given θ_D.

For the symmetric three-beam case with decision thresholds $\pm\tau$, and assuming the true AoD corresponds to the center beam (i.e., H_2), the error probability is:

$$P_{e|2}(\theta_D) = \Pr(|\text{DSR}| \ge \tau|H_2) = 2Q\left(\frac{\tau-\mu(\theta_D)}{\sigma(\theta_D)}\right), \tag{43}$$

where $Q(\cdot)$ is the complementary cumulative distribution function of the standard normal distribution [23].

Similarly, for the edge beams, the error probabilities are:

$$P_{e|1}(\theta_D) = \Pr(\text{DSR} < \tau|H_1) = \Phi\left(\frac{\tau-\mu(\theta_D)}{\sigma(\theta_D)}\right) \tag{44}$$

$$P_{e|3}(\theta_D) = \Pr(\text{DSR} > -\tau|H_3) = Q\left(\frac{-\tau-\mu(\theta_D)}{\sigma(\theta_D)}\right), \tag{45}$$

where $\Phi(\cdot)$ is the cumulative distribution function of the standard normal distribution [23].

The overall fine selection error probability is then the weighted average over all possible true AoD positions within the group:

$$\begin{aligned} P_{e,\text{fine}} &= \int_{\text{group}} p(\theta_D)P_{e,\text{fine}}(\theta_D)d\theta_D, \\ &= \frac{1}{2\Theta_M}\sum_{i=1}^{3}\int_{\theta_D\in H_i} P_{e|i}(\theta_D)d\theta_D, \end{aligned} \tag{46}$$

where $p(\theta_D)$ is the probability density function of the true AoD within the group.

The total beam selection error probability combines errors from both levels:

$$P_{e,\text{total}} = P_{e,\text{group}} + (1-P_{e,\text{group}})P_{e,\text{fine}}. \tag{47}$$

For high SNR conditions and $\text{SNR}_g > \max_{j\neq g}\text{SNR}_j$, from (28), we have $P_{e,\text{group}} \to 0$ exponentially fast. Therefore, the total error probability can be approximated as:

$$P_{e,\text{total}} \approx P_{e,\text{fine}} \quad \text{for high SNR.} \tag{48}$$

Remark 3: We note that the exhaustive codebook search algorithm also exhibits beam selection errors due to noise. The probability of selecting the jth beam when the optimal beam is the ith beam can be approximated using a similar approach as in Lemma 1. Specifically, the pairwise beam selection error probability can be approximated as

$$P_{i\to j}^{\text{exhaustive}} \approx Q\left(\frac{\text{SNR}_i - \text{SNR}_j}{\sqrt{2(\text{SNR}_i+\text{SNR}_j)}}\right), \tag{49}$$

where $\text{SNR}_j = \frac{P_t\rho_p|a^H(\theta_D)w_j|^2}{\sigma_n^2}$ and $\text{SNR}_i = \frac{P_t\rho_p|a^H(\theta_D)w_i|^2}{\sigma_n^2}$ are the effective SNRs for the ith and jth beams in the predefined beam set, respectively. Therefore, the beam selection error probability for the exhaustive codebook search algorithm can

then be derived as

$$P_{e,\text{exhaustive}} \approx \frac{1}{2\Theta_M}\int_{-\Theta_M}^{\Theta_M} Q\left(\frac{\text{SNR}_i - \max_{j\neq i}\text{SNR}_j}{\sqrt{2\left(\text{SNR}_i + \max_{j\neq i}\text{SNR}_j\right)}}\right) d\theta_D. \quad (50)$$

B. ANALYSIS ON AVERAGE HARVESTED ENERGY

From (8), the harvested energy depends on the selected beam. The expected harvested energy, $\mathbb{E}[E]$, is the average over all possible AoDs θ_D (assumed uniformly distributed, $p(\theta_D) = 1/(2\Theta_M)$) and all possible beam selections i^* given θ_D.

$$\mathbb{E}[E] \approx \frac{(K-K_p)\,T_s}{2\Theta_M}\int_{-\Theta_M}^{\Theta_M}\sum_{k=1}^{3}\left[\left(\frac{\Psi_k(\theta_D) - M_{\text{EH}}\,\Omega}{1-\Omega}\right) \times P(i^* = k \mid \theta_D)\right] d\theta_D, \quad (51)$$

where k indexes the beams within the selected group (assumed to be 3), $P(i^* = k \mid \theta_D)$ is the probability of selecting beam k given θ_D, and $\Psi_k(\theta_D)$ is the non-linear function from (9) evaluated using the input power $P_{\text{in},k} = P_t\rho_p|a^H(\theta_D)w_k|^2$ corresponding to the k-th beam.

V. OPTIMAL RESOURCE ALLOCATION

The non-linear nature of the harvested energy function in (51) complicates the optimization process. To gain analytical tractability, we introduce a linearized model for the harvested energy, which is particularly accurate in the low P_{in} regime. This approximation is well-suited for our analysis, as target applications like IoT networks typically operate within this low-power regime [24].

Lemma 2 (Linearized EH Model): For low input power, the non-linear harvested energy in (8) can be approximated by a linear function of P_{in}:

$$E_{i,\text{lin}} \approx (K-K_p)T_s \cdot \eta_{\text{lin}} \cdot P_{\text{in}}, \quad (52)$$

where $\eta_{\text{lin}} = a \cdot M_{\text{EH}} \cdot \Omega$ is the effective linear conversion efficiency, and $\Omega = (1+\exp(ab))^{-1}$ is a constant.

Proof: The non-linear term $\Psi = f(P_{\text{in}})$ is approximated using a first-order Taylor expansion around $P_{\text{in}} = 0$. We find $f(0) = M_{\text{EH}}\Omega$ and the derivative $f'(0) = aM_{\text{EH}}\Omega(1-\Omega)$. Substituting the approximation $\Psi_{\text{lin}} \approx f(0)+f'(0)P_{\text{in}}$ into (8) yields:

$$\begin{aligned} E_{i,\text{lin}} &\approx (K-K_p)T_s\left(\frac{(M_{\text{EH}}\Omega + aM_{\text{EH}}\Omega(1-\Omega)P_{\text{in}}) - M_{\text{EH}}\Omega}{1-\Omega}\right) \\ &= (K-K_p)T_s\left(\frac{aM_{\text{EH}}\Omega(1-\Omega)P_{\text{in}}}{1-\Omega}\right) \\ &= (K-K_p)T_s \cdot (aM_{\text{EH}}\Omega) \cdot P_{\text{in}}, \end{aligned}$$

which completes the proof. □

Using this linear model, the expected harvested energy $\mathbb{E}[E]$ in (51) can be approximated as:

$$\mathbb{E}[E] \approx \frac{\eta(K-K_p)T_sP_t\rho_p}{2\Theta_M}\sum_{k=1}^{3}\int_{-\Theta_M}^{\Theta_M} G_k P(i^* = k|\theta_D)d\theta_D. \quad (53)$$

Accordingly, from (22) and (53), the harvested energy depends on two competing factors as N_b increases: the training overhead $K_p = \lceil N_b/3 \rceil + 1$ grows, reducing the available time for energy transfer $(K - K_p)$, while the beamforming gain G_k and beam selection accuracy improve. This trade-off suggests an optimal value of N_b that maximizes the harvested energy.

The optimization problem can be formulated as:

$$N_b^* = \arg\max_{N_b} \mathbb{E}[E(N_b)], \quad (54)$$

where the dependency on N_b is explicitly shown. Substituting the training overhead from (22), we have

$$\mathbb{E}[E(N_b)] = \eta\,(K - \lceil N_b/3 \rceil - 1)\,T_sP_t\rho_p\bar{G}(N_b), \quad (55)$$

where $\bar{G}(N_b)$ represents the expected beamforming gain that depends on N_b through improved angular resolution and reduced beam selection error probability.

To analyze the concavity properties of the harvested energy function, we consider the continuous relaxation where $\lceil N_b/3 \rceil \approx N_b/3$ for large N_b. The harvested energy function becomes

$$\mathbb{E}[E(N_b)] \approx \eta\left(K - \frac{N_b}{3} - 1\right)T_sP_t\rho_p\bar{G}(N_b). \quad (56)$$

The following lemma establishes the concavity property of the harvested energy function.

Lemma 3: Under the assumption of uniform angular distribution and high SNR conditions, the harvested energy function $\mathbb{E}[E(N_b)]$ in (56) is concave in N_b for sufficiently large N_b.

Proof: To prove concavity, we need to show that the second derivative $\frac{d^2\mathbb{E}[E(N_b)]}{dN_b^2} < 0$ [25]. Taking the first derivative:

$$\frac{d\mathbb{E}[E(N_b)]}{dN_b} = \eta T_sP_t\rho_p\left[-\frac{1}{3}\bar{G}(N_b) + \left(K - \frac{N_b}{3} - 1\right)\frac{d\bar{G}(N_b)}{dN_b}\right], \quad (57)$$

where the expected beamforming gain $\bar{G}(N_b)$ increases with N_b due to improved angular resolution, but at a decreasing rate. For uniform linear arrays with sufficient oversampling, the beamforming gain follows approximately

$$\bar{G}(N_b) \approx G_{\max}\left(1 - C_1e^{-C_2N_b}\right), \quad (58)$$

where $G_{\max}$ is the maximum achievable gain, and C_1, $C_2 > 0$ are constants depending on the array geometry and

Algorithm 2 Bisection Algorithm for Optimal N_b Selection

Require: System parameters: K, η, T_s, P_t, ρ_p, tolerance ϵ
Require: Search bounds: $N_{b,\min}$, $N_{b,\max}$
Ensure: Optimal number of beams N_b^*
1: Initialize: $a \leftarrow N_{b,\min}$, $b \leftarrow N_{b,\max}$
2: **while** $b-a > \epsilon$ **do**
3: $c \leftarrow \lfloor (a+b)/2 \rfloor$
4: Compute $f'(c) = \left.\frac{d\mathbb{E}[E(N_b)]}{dN_b}\right|_{N_b=c}$
5: **if** $f'(c) > 0$ **then**
6: $a \leftarrow c$ ▷ Optimum is in the right half
7: **else**
8: $b \leftarrow c$ ▷ Optimum is in the left half
9: **end if**
10: **end while**
11: $N_b^* \leftarrow \lfloor (a+b)/2 \rfloor$ **return** N_b^*

angular distribution. This gives

$$\frac{d\bar{G}(N_b)}{dN_b} = G_{\max} C_1 C_2 e^{-C_2 N_b} \tag{59}$$

$$\frac{d^2\bar{G}(N_b)}{dN_b^2} = -G_{\max} C_1 C_2^2 e^{-C_2 N_b} < 0. \tag{60}$$

Taking the second derivative of the harvested energy

$$\frac{d^2\mathbb{E}[E(N_b)]}{dN_b^2} = \eta T_s P_t \rho_p \left[-\frac{2}{3}\frac{d\bar{G}(N_b)}{dN_b} + \left(K - \frac{N_b}{3} - 1\right)\frac{d^2\bar{G}(N_b)}{dN_b^2} \right]. \tag{61}$$

From (59) and (60), for sufficiently large N_b, both $\frac{d\bar{G}(N_b)}{dN_b}$ and $\frac{d^2\bar{G}(N_b)}{dN_b^2}$ approach zero, ensuring $\frac{d^2\mathbb{E}[E(N_b)]}{dN_b^2} < 0$ and therefore, proving the concavity of $\mathbb{E}[E(N_b)]$. □

Given the concavity property established in Lemma 3, we can use the bisection method to find the optimal N_b^*. The algorithm searches for the point where $\frac{d\mathbb{E}[E(N_b)]}{dN_b} = 0$, which is summarized in Algorithm 2. The derivative computation in line 4 of Algorithm 2 can be approximated numerically as:

$$f'(c) \approx \frac{\mathbb{E}[E(c+1)] - \mathbb{E}[E(c-1)]}{2}, \tag{62}$$

where $\mathbb{E}[E(N_b)]$ is computed using (55) with the expected beamforming gain estimated from system parameters.

VI. SIMULATION RESULTS AND PERFORMANCE EVALUATION

We evaluate the performance of the proposed two-level beam selection algorithm through extensive Monte Carlo simulations. The system parameters are summarized in Table 1. We note that, unless otherwise stated, the parameters for the nonlinear EH model is set as $a = 150$, $b = 0.014$, and $M_{EH} = 24$ mW, which is obtained by curve-fitting of the measurement data from [22], [26].

TABLE 1. Simulation parameters.

Parameter	Value
Number of antennas (M)	12, 18
Number of beams (N_b)	24, 36
Angular range	$[-60^o, 60^o]$
Antenna spacing (d)	$\lambda/2$
Frame duration (K)	100 time slots
Transmit power (P_t)	-20:4:20 dBm
Noise power (σ_n^2)	-20 dBm
Parameters for nonlinear EH model in (8)	$a = 150$, $b = 0.014$, $M_{\text{EH}} = 24$ mW
Group size (L)	3

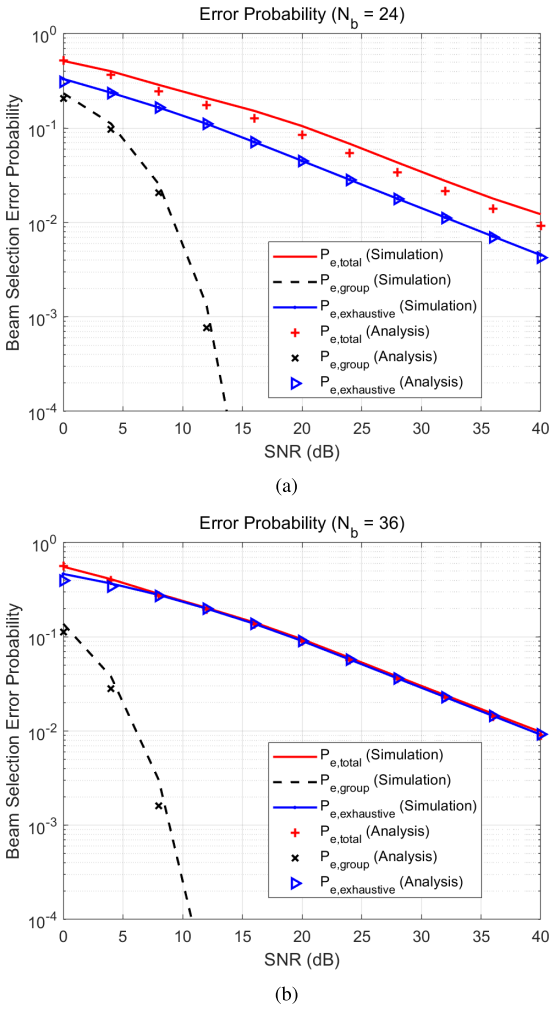

FIGURE 4. Beam selection error probability for various SNRs when (a) $N_b = 24$ (b) $N_b = 36$ with $M = 12$.

We compare the proposed algorithm with the conventional exhaustive codebook search method as a baseline. The key performance metrics include beam selection accuracy and average harvested energy. We also validate the performance of the optimal resource allocation algorithm in Section V.

A. BEAM SELECTION ERROR PROBABILITY

In Fig. 4, the beam selection error probabilities are evaluated when (a) $N_b = 24$ (b) $N_b = 36$ with $M = 12$. We note that,

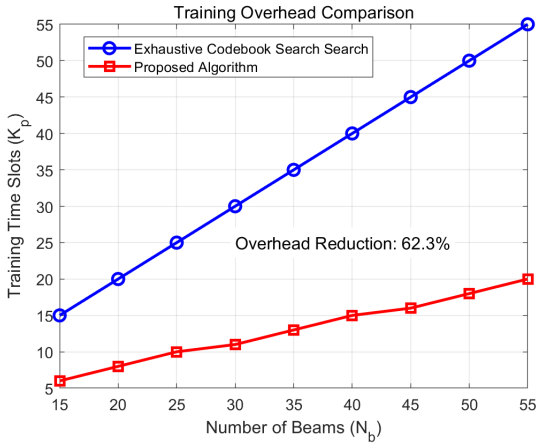

FIGURE 5. Training overhead comparison for various N_b.

as SNR increases, the overall beam selection error decreases. In addition, as discussed in Section IV-A2, the group selection error probability decreases exponentially fast. The proposed two-level algorithm exhibits similar or slightly worse error performance compared to the exhaustive codebook search.

B. TRAINING OVERHEAD ANALYSIS

In Fig. 5, the time slots required for the beam training are evaluated for the proposed two-level beam selection algorithm and the exhaustive codebook search algorithm. From the figure, the training overhead reduction achieved by the proposed algorithm is approximately 62.3 % on average. For example, when $N_b = \{15, 40\}$, the proposed algorithm requires only 6 and 15 training slots compared to $\{15, 40\}$ slots for exhaustive codebook search, resulting in 60 % and 62.5 % overhead reduction, respectively. From Figs. 4 and 5, the proposed two-level beam selection algorithm achieves significant reduction in training overhead without degradation in the beam selection error probability.

C. ENERGY HARVESTING PERFORMANCE

In Fig. 6, the normalized harvested energy (i.e., the harvested energy divided by the transmit power given by E/P_t) is evaluated when $N_b = \{24, 36\}$. From (8) and Lemma 2, the normalized harvested energy is given as a function of K_p and the beamforming gain. From Fig. 6(a), due to the beam selection error at low SNR (less than 5 dB), the proposed algorithm exhibits lower harvested energy than the exhaustive codebook search algorithm. In contrast, at high SNR, the proposed algorithm outperforms the exhaustive codebook search algorithm. From Fig. 6(b), when $N_b = 36$, the proposed algorithm consistently achieves higher harvested energy than exhaustive codebook search. This superior performance stems from the reduced training overhead, which allocates more time slots for actual power transfer. In Fig. 7, the energy efficiency ratio for various SNRs is evaluated when $N_b = \{24, 36\}$. From the figure, at high SNR, the proposed two-level beam selection method can

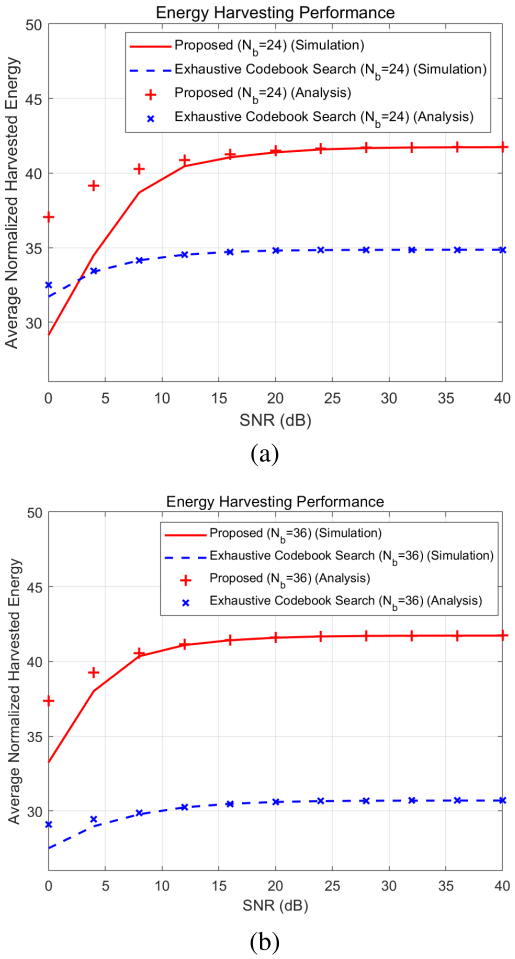

FIGURE 6. Normalized harvested energy for various SNRs when (a) $N_b = 24$ (b) $N_b = 36$.

achieve approximately $\{20, 35\}$ percent improvement for $N_b = \{24, 36\}$ in the harvested energy, respectively.

D. OPTIMAL RESOURCE ALLOCATION RESULTS

Fig. 8 shows the harvested energy as a function of N_b for different frame durations K. The results confirm the concave nature of the harvested energy function and validate the effectiveness of the proposed bisection algorithm (i.e., Algorithm 2) in finding the optimal N_b^*. For $K = 80$, the optimal N_b^* is approximately 25, while for $K = 250$, it increases to around 40, demonstrating the dependency on system parameters. In addition, due to the increased energy harvesting time, $K = 250$ exhibits higher harvested energy than $K = 80$. In Fig. 9, the convergence of Algorithm 2 is validated when $K = \{80, 250\}$ and $M = 12$. It can be found that the normalized harvested energy converges to the maximum value in four iterations.

To further validate the effectiveness of the proposed algorithm, we compare it with the adaptive hierarchical beam search baseline, inspired by the IEEE 802.11ad/ay standards [9], [15]. The adaptive method employs a

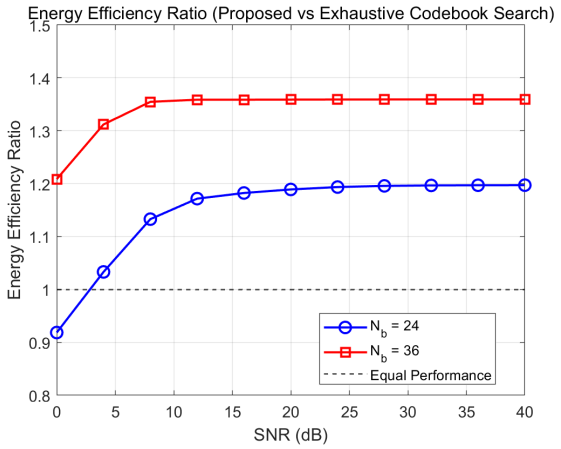

FIGURE 7. Energy efficiency ratio for various SNRs when $N_b = \{24, 36\}$.

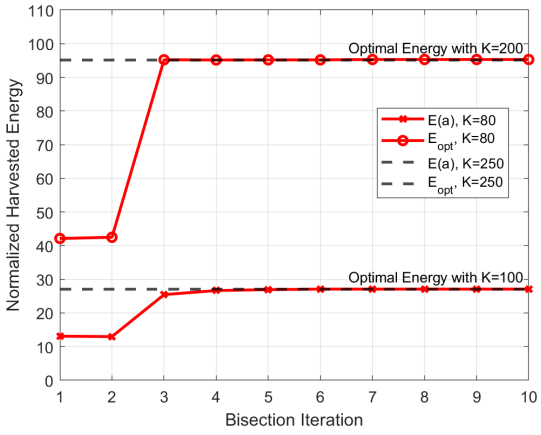

FIGURE 9. Normalized harvested energy over iterations in Algorithm 2 when $K = \{80, 250\}$.

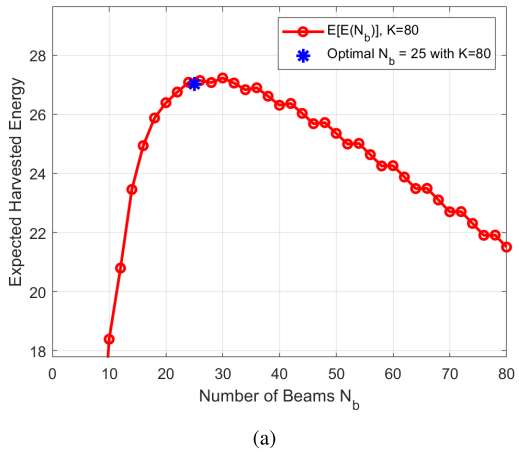

FIGURE 8. Normalized harvested energy for various N_b when (a) $K = 80$ and (b) $K = 250$.

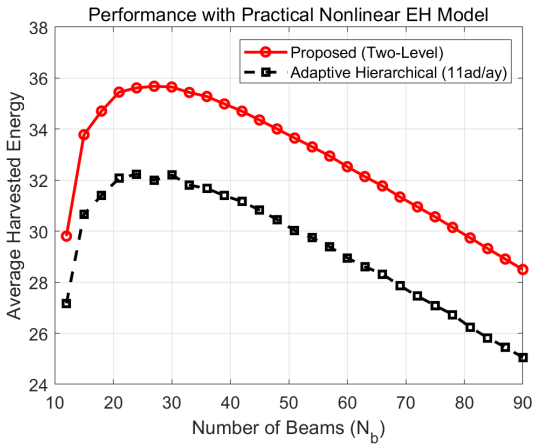

FIGURE 10. Normalized harvested energy for various N_b with $K = 100$.

multi-resolution codebook search, consisting of a coarse sector sweep followed by $S = 4$ stages of binary refinement. As illustrated in Fig. 10, the proposed two-level algorithm consistently outperforms the adaptive hierarchical method in terms of average harvested energy across the entire range of N_b. This is because the accumulated training overhead (approximately $N_g + 2S$ slots) significantly reduces the time remaining for energy harvesting within a fixed frame duration K. Furthermore, the proposed method utilizes the difference-to-sum ratio (DSR) to achieve fine-grained selection in a single additional time slot, whereas the adaptive method requires multiple measurements at each refinement level. These results demonstrate that the proposed algorithm strikes a superior balance between training efficiency and energy harvesting performance, making it more suitable for power-constrained mmWave WPT environments where minimizing training overhead is critical.

VII. CONCLUSION

This paper presented a novel two-level beam selection algorithm for mmWave WPT systems that significantly reduces training overhead while maintaining near-optimal energy harvesting performance. The algorithm employs a hierarchical approach using sum and difference beams inspired by monopulse radar techniques. The comprehensive

analytical framework using detection theory and order statistics provides theoretical insights into the algorithm's performance. From the analytic results, the bisection algorithm to find the optimal number of beams (which determines the beam training period) is also proposed such that the harvested energy is maximized. Simulation results confirm that the proposed two-level beam selection algorithm achieves higher harvested energy compared to conventional exhaustive codebook search methods by reducing training time from N_b to approximately $\lceil N_b/3 \rceil + 1$ time slots. Furthermore, given the system parameters, the optimal number of beams can be effectively found by using the proposed bisection-based optimization algorithm.

APPENDIX
PROOF OF LEMMA 1

Proof:

Let us define the received signal powers as $Z_g = |y_{\Sigma,g}|^2$ and $Z_j = |y_{\Sigma,j}|^2$. Given the complex Gaussian nature of the received signals, we have

$$y_{\Sigma,g} = \sqrt{P_t \rho_p} a^H(\theta_D) w_{\Sigma,g} s + n_g \tag{63}$$

$$y_{\Sigma,j} = \sqrt{P_t \rho_p} a^H(\theta_D) w_{\Sigma,j} s + n_j, \tag{64}$$

where n_g and n_j are independent complex Gaussian random variables with zero mean and variance σ_n^2. Under hypothesis H_g (i.e., θ_D belongs to group g), the received signal power follows non-central chi-squared distribution with non-centrality parameter $\lambda_g = \frac{2P_t \rho_p |a^H(\theta_D) w_{\Sigma,g}|^2}{\sigma_n^2} = 2\text{SNR}_g$. Specifically,

$$Z_g \sim \chi_2^2(\lambda_g). \tag{65}$$

The probability density function is then given as:

$$f_{Z_g}(z) = \frac{1}{\sigma_n^2} exp\left(-\left(\frac{z}{\sigma_n^2} + \frac{\lambda_g}{2}\right)\right) I_0\left(\sqrt{\frac{2\lambda_g z}{\sigma_n^2}}\right) \tag{66}$$

Similarly, $Z_j \sim \chi_2^2(\lambda_j)$ with $\lambda_j = \frac{2P_t \rho_p |a^H(\theta_D) w_{\Sigma,j}|^2}{\sigma_n^2} = 2\text{SNR}_j$.

For the high SNR case where $\lambda_g, \lambda_j \gg 1$, the non-central chi-squared distribution can be approximated by a Gaussian distribution [27]. Specifically,

$$Z_g \approx \mathcal{N}(\sigma_n^2(1 + \lambda_g/2), \sigma_n^4(\lambda_g + 1)) \tag{67}$$

$$Z_j \approx \mathcal{N}(\sigma_n^2(1 + \lambda_j/2), \sigma_n^4(\lambda_j + 1)). \tag{68}$$

Therefore, the difference $Z_j - Z_g$ follows a Gaussian distribution with:

$$\mathbb{E}[Z_j - Z_g] = \frac{\sigma_n^2}{2}(\lambda_j - \lambda_g) \tag{69}$$

$$\text{Var}(Z_j - Z_g) = \sigma_n^4(\lambda_j + \lambda_g + 2) \tag{70}$$

The probability of incorrectly selecting group j instead of group g is then derived as

$$P_{g\to j} = \Pr(Z_j - Z_g > 0) = Q\left(\frac{-\sigma_n^2(\lambda_j - \lambda_g)}{\sqrt{4\sigma_n^4(2 + \lambda_g + \lambda_j)}}\right). \tag{71}$$

Here, the argument of the Q-function can be simplified as

$$\frac{-\sigma_n^2(\lambda_j - \lambda_g)}{\sqrt{4\sigma_n^4(2 + \lambda_g + \lambda_j)}} = \frac{(\lambda_g - \lambda_j)}{2\sqrt{2 + \lambda_g + \lambda_j}} = \frac{(\text{SNR}_g - \text{SNR}_j)}{\sqrt{2(1 + \text{SNR}_g + \text{SNR}_j)}}, \tag{72}$$

which completes the proof. We note that the noise variance σ_n^2 cancels out in the final expression, leaving only the SNR ratio terms. This is expected from a physical standpoint, as the error probability should depend only on the relative signal strengths, not the absolute noise power. □

REFERENCES

[1] Z. Zhang, H. Pang, A. Georgiadis, and C. Cecati, "Wireless power transfer—An overview," *IEEE Trans. Ind. Electron.*, vol. 66, no. 2, pp. 1044–1058, Feb. 2019.
[2] M. Molefi, E. D. Markus, and A. Abu-Mahfouz, "Wireless power transfer for IoT devices—A review," in *Proc. Int. Multidisciplinary Inf. Technol. Eng. Conf. (IMITEC)*, Nov. 2019, pp. 1–8.
[3] M. Wagih, A. S. Weddell, and S. Beeby, "Millimeter-wave power harvesting: A review," *IEEE Open J. Antennas Propag.*, vol. 1, pp. 560–578, 2020.
[4] J. Guo, X. Zhou, and S. Durrani, "Wireless power transfer via mmWave power beacons with directional beamforming," *IEEE Wireless Commun. Lett.*, vol. 8, no. 1, pp. 17–20, Feb. 2019.
[5] T. A. Khan and R. W. Heath Jr., "Wireless power transfer in millimeter wave tactical networks," *IEEE Signal Process. Lett.*, vol. 24, no. 9, pp. 1284–1287, Sep. 2017.
[6] S. Wang and S. Bi, "Improving beam alignment accuracy in mmWave communication systems with auxiliary tasks," *IEEE Signal Process. Lett.*, vol. 30, pp. 992–996, 2023.
[7] F. Laue, M. Garkisch, V. Jamali, and R. Schober, "Performance tradeoff of RIS beam training: Overhead vs. achievable SNR," in *Proc. 56th Asilomar Conf. Signals, Syst., Comput.*, Oct. 2022, pp. 408–412.
[8] S. Noh, M. D. Zoltowski, and D. J. Love, "Multi-resolution codebook and adaptive beamforming sequence design for millimeter wave beam alignment," *IEEE Trans. Wireless Commun.*, vol. 16, no. 9, pp. 5689–5701, Sep. 2017.
[9] T. Nitsche, C. Cordeiro, A. B. Flores, E. W. Knightly, E. Perahia, and J. C. Widmer, "IEEE 802.11ad: Directional 60 GHz communication for multi-gigabit-per-second Wi-Fi [Invited paper]," *IEEE Commun. Mag.*, vol. 52, no. 12, pp. 132–141, Dec. 2014.
[10] J. Choi, "Beam selection in mm-wave multiuser MIMO systems using compressive sensing," *IEEE Trans. Commun.*, vol. 63, no. 8, pp. 2936–2947, Aug. 2015.
[11] J. Chen, W. Feng, J. Xing, P. Yang, G. E. Sobelman, D. Lin, and S. Li, "Hybrid beamforming/combining for millimeter wave MIMO: A machine learning approach," *IEEE Trans. Veh. Technol.*, vol. 69, no. 10, pp. 11353–11368, Oct. 2020.
[12] G. Raja, M. R. Kanagarathinam, D. S. Rajendran, S. V. Ravuru, S. Mamalaivasan, and S. Singh, "OBSDNN: Optimal beam selection employing deep neural networks in 6G environment," in *Proc. IEEE Globecom Workshops (GC Wkshps)*, Dec. 2024, pp. 1–6.
[13] M. Zecchin, M. B. Mashhadi, M. Jankowski, D. Gündüz, M. Kountouris, and D. Gesbert, "LiDAR and position-aided mmWave beam selection with non-local CNNs and curriculum training," *IEEE Trans. Veh. Technol.*, vol. 71, no. 3, pp. 2979–2990, Mar. 2022.
[14] A. Alkhateeb, S. Alex, P. Varkey, Y. Li, Q. Qu, and D. Tujkovic, "Deep learning coordinated beamforming for highly-mobile millimeter wave systems," *IEEE Access*, vol. 6, pp. 37328–37348, 2018.
[15] K. Aldubaikhy, W. Wu, N. Zhang, N. Cheng, and X. Shen, "mmWave IEEE 802.11ay for 5G fixed wireless access," *IEEE Wireless Commun.*, vol. 27, no. 2, pp. 88–95, Apr. 2020.
[16] B. R. Mahafza, *Radar Systems Analysis and Design Using MATLAB*. Boca Raton, FL, USA: CRC Press, 2005.
[17] A. F. Morabito and P. Rocca, "Optimal synthesis of sum and difference patterns with arbitrary sidelobes subject to common excitations constraints," *IEEE Antennas Wireless Propag. Lett.*, vol. 9, pp. 623–626, 2010.

[18] A. F. Morabito and P. Rocca, "Reducing the number of elements in phase-only reconfigurable arrays generating sum and difference patterns," *IEEE Antennas Wireless Propag. Lett.*, vol. 14, pp. 1338–1341, 2015.
[19] J. Park, J. Lee, J. Chun, and S. Kwak, "Robust monopulse beam synthesis with sparse elements in linear and planar arrays with element failure detection," *IET Radar, Sonar Navigat.*, vol. 11, no. 8, pp. 1251–1258, Aug. 2017.
[20] F. Cai, H. Fan, Z. Song, and Q. Fu, "Difference beam aided target detection in monopulse radar," *Chin. J. Aeronaut.*, vol. 28, no. 5, pp. 1485–1493, Oct. 2015.
[21] E. Boshkovska, D. W. K. Ng, N. Zlatanov, and R. Schober, "Practical non-linear energy harvesting model and resource allocation for SWIPT systems," *IEEE Commun. Lett.*, vol. 19, no. 12, pp. 2082–2085, Dec. 2015.
[22] Y. Wang, Y. Wang, F. Zhou, Y. Wu, and H. Zhou, "Resource allocation in wireless powered cognitive radio networks based on a practical non-linear energy harvesting model," *IEEE Access*, vol. 5, pp. 17618–17626, 2017.
[23] J. L. Devore, *Probability and Statistics*. Pacific Grove, CA, USA: Brooks/Cole, 2000.
[24] X. Lu, P. Wang, D. Niyato, D. I. Kim, and Z. Han, "Wireless networks with RF energy harvesting: A contemporary survey," *IEEE Commun. Surveys Tuts.*, vol. 17, no. 2, pp. 757–789, 2nd Quart., 2015.
[25] S. Boyd and L. Vandenberghe, *Convex Optimization*, 7th ed., New York, NY, USA: Cambridge Univ. Press, 2009.
[26] J. Guo and X. Zhu, "An improved analytical model for RF-DC conversion efficiency in microwave rectifiers," in *IEEE MTT-S Int. Microw. Symp. Dig.*, Jun. 2012, pp. 1–3.
[27] D. Horgan and C. C. Murphy, "On the convergence of the chi square and noncentral chi square distributions to the normal distribution," *IEEE Commun. Lett.*, vol. 17, no. 12, pp. 2233–2236, Dec. 2013.

SEUNGSU CHUNG received the B.S. degree in electronic engineering from Pukyong National University, South Korea, in 2025, where he is currently pursuing the M.S. degree with the Department of Electronic Engineering. His research interests include radar signal processing, FMCW radar systems, communication signal processing, wireless power transfer, and beam index tracking using monopulse beamforming

JAEYEON HA is currently pursuing the B.S. degree with the Department of Electronic Engineering, Pukyong National University, South Korea. His research interests include radar signal processing, FMCW radar systems, communication signal processing, sonar signal processing, and GNU radio systems.

JAEHYUN PARK (Member, IEEE) received the B.S. and Ph.D. (M.S.-Ph.D. joint program) degrees in electrical engineering from Korea Advanced Institute of Science and Technology (KAIST), in 2003 and 2010, respectively. From 2010 to 2013, he was a Senior Researcher at the Electronics and Telecommunications Research Institute (ETRI), where he worked on transceiver design and spectrum sensing for cognitive radio systems. From 2013 to 2014, he was a Postdoctoral Research Associate at the Electrical and Electronic Engineering Department, Imperial College London. He is currently a Professor with the Electronic Engineering Department, Pukyong National University, South Korea. His research interests include signal processing for wireless communications and radar systems, with a focus on detection and estimation for MIMO systems, MIMO radar, cognitive radio networks, and joint information and energy transfer.

JAE CHEOL PARK received the B.S. degree in electronics engineering and the M.S.E. degree in electronics and radio engineering from Kyung Hee University, in 2009 and 2010, respectively, and the Ph.D. degree in electrical engineering from KAIST, in 2024. He is currently a Principal Researcher with ETRI. His research interests include the design and analysis of UAV communication systems, machine learning for wireless communication systems, and mmWave communication systems.

JUNGICK MOON (Member, IEEE) received the M.S. and Ph.D. degrees in electrical engineering from the Department of Electrical Engineering, KAIST, Daejeon, South Korea, in 2000 and 2004, respectively. Since 2004, he has been with ETRI as a Principal Researcher. His research interests include small and broadband antennas, wireless power transmission, and RF energy harvesting technologies.